"Synthesis and triplex-forming properties of cyclic oligonucleotides with G,A-antiparallel strands." Grimau, M.G., Gargallo, R., Aviñó, A., Eritja, R. Chem. Biodiv., 2(2), 275-285 (2005). doi: 10.1002/cbdv.200590010

Synthesis and Triplex-Forming Properties of Cyclic Oligonucleotides with G,A-Antiparallel Strands.

by **Marta G. Grimau[a]), Anna Aviñó[a]), Raimundo Gargallo[b])** and **Ramon Eritja[*a]).**

[a]) Department of Structural Biology. Institut de Biologia Molecular de Barcelona. C.S.I.C., Jordi Girona 18-26, E-08034 Barcelona. Spain. (phone: +34(93)4006145; fax: +34(93)2045904; e-mail : recgma@cid.csic.es)

[b]) Department of Analytical Chemistry. Universitat de Barcelona. Martí i Franqués 1-11, E-08028 Barcelona, Spain.

Cyclic oligonucleotides carrying an oligopurine Watson-Crick sequence linked to the corresponding (G,A)-and (G,T)-antiparallel strands were prepared by nonenzymatic template-assisted cyclization of phosphorylated precursors. Cyclization was attempted using 3'-phosphate and 5'-phosphate linear precursors with carbodiimide or BrCN activation. The best results were obtained with the 5'-phosphorylated precursors and carbodiimide activation. Cyclic oligonucleotides bind polypyrimidine target sequence by formation of antiparallel triplexes. We have used UV and circular dichroism (CD) spectroscopy to analyze triplexes formed by cyclic oligonucleotides carrying G and A in the reverse Hoogsteen strand. The relative stability of the triplexes formed by cyclic and linear oligonucleotides with a common polypyrimidine target was determined using melting experiments. The most stable triplexes were formed by the cyclic oligonucleotide followed by the unphosphorylated and phosphorylated oligonucleotide precursors and, finally, the corresponding hairpin. Although the differences in binding affinity between cyclics and their corresponding linear precursors are small, the use of cyclics offers a clear advantage over conventional duplex recognition.

Introduction.- Currently, there is increasing interest in the design of sequence-specific DNA- and RNA-binding molecules that may have diagnostic or therapeutic uses. Thus, certain oligonucleotides have been shown to bind oligopurine-oligopyrimidine sequences of double-stranded DNA by forming triple-helical structures (triplexes, Scheme 1) [1-3]. Depending on the orientation of the third strand with respect to the central oligopurine Watson-Crick strand, triplexes are classified into two main categories: (i) parallel and (ii) antiparallel. The formation of parallel triplexes usually requires protonation of N3 of cytosine to undergo correct Hoogsteen bonding with

N7 of guanine; for this reason they are most stable under acidic conditions. In contrast, antiparallel triplexes do not require protonation to form the reverse Hoogsteen H-bonds [1-3].

An alternative approach to the generation of oligonucleotide-derived DNA-, or RNA-binding molecules is based on triplex formation via the linkage of one Watson-Crick strand with the third strand or triplex forming oligonucleotide (TFO) (Scheme 1). Such DNA hairpins bind single-stranded nucleic acids targets by triplex formation [4-5]. This strategy has been further developed to bind double-stranded DNA by strand displacement using PNA derivatives. In this case, the driving force is the high stability of PNA-PNA-DNA triplexes [6-7].

Cyclic oligonucleotides designed to form triplexes have also been shown to bind target single-stranded DNA and RNA targets with affinities and sequence selectivities that are considerably higher than those seen for the corresponding hairpins [8-9]. However, most of this work has been undertaken using T-/C-rich cyclic oligonucleotides designed to bind the polypurine Watson-Crick strand [8, 9]. In contrast, there is little information available on purine-rich cyclic oligonucleotides designed to bind the polypyrimidine Watson-Crick strand, and available data has been obtained with cyclic oligonucleotides carrying the (G,T)-antiparallel strand [10-12].

Here we describe the synthesis and properties of oligonucleotides containing the oligopurine Watson-Crick strand linked to the (G,A)-antiparallel strand by one or two loops. The results obtained show that cyclic oligonucleotides carrying (G,A)-antiparallel strands can be obtained in good yields via template-assisted cyclization of 5'-phosphorylated linear precursors. Moreover, triplex formation between these oligonucleotides and their target can be monitored by UV and CD-spectroscopy. The binding affinity of the cyclic oligonucleotide carrying (G,A)-reverse antiparallel strands is 8 kcal/mol more stable than conventional duplex recognition.

Results. - *1. Synthesis of 3'-phosphate and 5'-phosphate precursors.* The target polypyrimidine sequence was selected from a triplex studied by Xodo et al [13, 14]. The same sequence has been

used to characterize the binding properties of both parallel [15] and antiparallel hairpins [16] (Scheme 2). We selected one of the phosphates in the middle of the Watson-Crick oligopurine sequence to disconnect the cyclic oligonucleotide (indicated in bold in Scheme 2) and design the sequence of the linear precursors. Oligonucleotides **1**-**4** (*Table 1*) with phosphate groups at either the 5'- (**1**, **2**) or 3'-end (**3**, **4)**, were prepared using phosphoramidite and a solid support derived from (4,4'-dimethoxytrityloxyethyl) hydroxyethyl sulfone [17]. 5'-Phosphorylated oligonucleotides were purified by HPLC using XTerra® columns. These columns allow the separation of 5'-phosphorylated oligonucleotides from non-phosphorylated sequences **5** and **6** (*Figure 1*). During the preparation of the 3'-phosphorylated oligonucleotide, we observed lower yields than expected. We suspect that the ammonia treatment was not efficient in breaking the bond between the 3'-phosphate and the solid support. Several treatments were assayed including longer times, use of 1,8-diazabicyclo[5.4.0]undec-7-ene (DBU) and use of a 1: 1 mixture of 40% methylamine and *conc*. ammonia. The best results were obtained by overnight treatment with the methylamine/ammonia mixture. Although the use of methylamine is not compatible with the use of the cytidine protected with the benzoyl group [18, 19], in our case this was not a problem, because the sequence did not contain cytidine. The 3'-phosphorylated oligonucleotide was purified by reverse-phase HPLC using a trityl-on protocol. The resulting product displayed a single peak in HPLC with XTerra® columns (data not shown).

2. Cyclization of phosphorylated precursors. Templated cyclization of phosphorylated precursors was studied using 1-(3-dimethylaminopropyl)-3-ethylcarbodimide (EDC) [20] or BrCN [10, 11, 20] as condensing agents. In our hands, 3'-phosphorylated sequences yielded very low amounts of cyclic oligonucleotides (less than 5%) using the conditions described in the literature. This lack of success may be due to the shorter length of the duplex part of the oligonucleotide and the fact that phosphate formation between purines is more difficult than between pyrimidines [20]. In contrast,

cyclization of 5'-phosphorylated sequences by EDC or BrCN generated a new product that migrated at a rate 0.9 times that of the linear precursor in polyacrylamide gel electrophoresis (PAGE). This product was resistant to digestion with a mixture of snake venom phosphodiesterase and alkaline phosphatase, and displayed the expected molecular weight in mass spectrometry (MALDI-TOF). Cyclization of oligonucleotide **2** with EDC represented the best reaction (70-90% conversion to cyclic oligonucleotide, as estimated by PAGE and HPLC using XTerra®; *Figure 2*). Conversion of sequence **1** to cyclic oligonucleotide **7** by EDC resulted in lower, but still good, yields (50-70% yield). The recovery of cyclic oligonucleotides from BrCN-catalyzed reactions was poor, due to the formation of a precipitate. This precipitation is explained by the formation of an insoluble complex with Ni^{2+} ions present in the BrCN reaction. Consequently, we isolated the reaction products from BrCN reactions by centrifugation of the reaction mixtures and dissolution of the pellets in a 0.1M EDTA solution. In this way, Ni^{2+} ions were complexed by EDTA and purine-containing oligonucleotides became soluble. Analysis of the BrCN-reactions show less than 50% conversion of linear to cyclic oligonucleotides. EDC-mediated cyclization did not produce any precipitate, and yields were better, consequently, this method was preferred. The desired cyclic oligonucleotides **7** and **8** were purified by either gel electrophoresis or HPLC using an XTerra® column (*Figure 2*).

3. *Melting experiments*. The binding properties of cyclic oligonucleotides **7** and **8** as well their phosphorylated and unphosphorylated linear sequences were analyzed by thermal denaturation with UV spectroscopy at pH 7.2. Hairpin sequences **9** and **10** were included for comparison as well as control oligonucleotides **11** and **12** with scrambled antiparallel strands [16]. Also, the complementary purine sequence **13,** without any antiparallel strand, was prepared. Melting studies of oligonucleotides **1-14** alone did not show any clear transition. In some cases, small changes could be observed at around 30-40 degrees, but they were not cooperative. This is due either to a

lack of secondary structure (oligonucleotides **11-14**) or to the absence of hyperchromicity observed during the dissociation of triplex forming strand in these sequences (oligonucleotides **1-10**) [16, 21, 22].

Melting experiments with complexes of oligonucleotides **1-13** and the target pyrimidine sequence **14** showed a clear transition, demonstrating that oligonucleotides **1-10** bind their target with a higher efficiency than their complementary and control sequences **11-13** (*Table 2)*. Cyclic oligonucleotide **8** bound the target with the highest stability (ΔG_{37} –19.1 Kcal/mol; *Table 2*). This represents an enhancement of 8 Kcal/mol over the simple Watson-Crick recognition (**13** ΔG_{37} –11.2 Kcal/mol, **12** ΔG_{37} -10.8 Kcal/mol; *Table 2*). Non-phosphorylated linear sequence **6** is slightly less stable (ΔG_{37} –17.5 Kcal/mol; *Table 2*). The presence of the phosphate in the linear sequence induces little or not destabilization of the triplex (**4** ΔG_{37} -17.5 and **2** ΔG_{37} –15.2 Kcal/mol; *Table 2*), and the triplex formed by hairpin **10** is approx. 3 Kcal/mol less stable (**10** ΔG_{37} –15.5 Kcal/mol; *Table 2*). It is important to note that the melting temperature of the hairpin is the highest of this series, but that the free energy inverts the order of relative stability. It has already been pointed out that melting temperatures are not always indicative of relative stability [23]. In some cases, differences in the shape of the melting curves means that a structure with a higher T_m will exhibit a lower stability [23]. In the present case, the melting curves of the hairpins and cyclic oligonucleotides have a similar T_m but the differences in the shape of the curves are responsible for the relative stability of the triplexes.

Similar results were obtained in the series carrying G,T-reverse Hoogsteen strand (*Table 3*). However, unfortunately, cyclic oligonucleotides **7** gave a broad curve with low hyperchromicity, and curve fitting was not possible in this particular case. Although thermodynamic parameters could not be obtained, cyclic oligonucleotide **7**, as well as linear and hairpin sequences **5**, **3**, **1**, and **9** displayed the highest T_m (54.9-58.5) and were at least 3.5-6.4 kcal/mol more stable than the simple Watson-Crick recognition (**5**, **3, 9**, and **5** ΔG_{37} –17.6, –15.7, -14.7, and -15.4 Kcal/mol respectively

Table 3; **11** ΔG_{37} -11.2 Kcal/mol, *Table 3*; **13** ΔG_{37} –11.2 Kcal/mol, *Table 2*). These results are in agreement with previous work on cyclic oligonucleotides carrying a (G,T)-reverse Hoogsteen strand [10, 11].

We have also run melting experiments in buffers containing NaCl and KCl instead of $MgCl_2$ in order to check whether G-quartet structures may inhibit triplex formation [24] but only a 8ºC decrease on Tm was observed (similar to parallel triplexes [15]) indicating no interference of these structures on triplex formation (data not shown).

The circular dichroism spectra of cyclic oligonucleotide **8** with and without target sequence **14** are shown in *Figure 3*. The CD spectrum of the triplex formed by an equimolar mixture of oligonucleotides **8** and **14** shows a positive band at 270 nm and a negative band at 242 nm. This spectrum is in agreement with the CD spectra of (G,A)-antiparallel triplexes described in literature [25]. Thermal denaturation of triplexes was also followed by CD spectroscopy. *Figure 4* shows the changes in the CD spectrum for the (G,A)-antiparallel triplex formed by oligonucleotides **8** and **14**. Analysis of the complete data set by multivariate curve resolution (MCR, [22, 26, 27]) revealed the presence of two species with a melting temperature of 51.5ºC (*Table 2*). The pure spectra of folded and unfolded structures resolved by MCR and the concentration profiles of both species are shown in *Figure 4*. The same methodology was applied to the analysis of the thermal denaturation of the (G,A)-antiparallel triplex formed by oligonucleotides **3** and **14**, giving a melting temperature of 52 ºC (*Table 2*). Although the melting temperatures obtained by UV- and CD-spectroscopy are in agreement, there is a difference of 5-7 degrees between the two methods. These differences are probably due to differences in the heating process employed; whilst heating is continuous in UV melting curves, the CD method uses steps of temperature with a waiting time for equilibration. Thermal denaturation of oligonucleotide **3** alone was also assessed by CD spectroscopy (data not shown). Here, a transition between two species was also observed, with a melting temperature of 33 ºC. This indicates that oligonucleotide **3** is partially folded, most probably forming reverse

Hoogsteen bonds, although UV-spectroscopy did not show changes during thermal denaturation of this oligonucleotide [16, 21, 22].

Discussion. The ability of cyclic oligonucleotides to bind single-stranded nucleic acid sequences by triplex formation has attracted a widespread interest due to the higher binding affinity and selectivity, as well as the enhanced resistance to exonuclease degradation [8, 9]. Here, we present for first time the synthesis and binding properties of a cyclic oligonucleotide designed to form (G,A)-antiparallel triplexes. These results complement other studies undertaken using cyclic oligonucleotides designed to form (G,T)-antiparallel triplexes [10, 11] and (C,T)-parallel triplexes [8, 9]. We show that cyclic oligonucleotides carrying (G,A)-antiparallel strands are obtained in good yields, probably due to a higher affinity to the template pyrimidine strand. The cyclic oligonucleotides obtained in this study have a high affinity to their polypyrimidine targets at neutral pH, making them interesting tools for antisense inhibition of gene expression.

It is important to note that previous work with antiparallel triplexes using (G,A)- and (G,T)-oligonucleotides and duplex DNA as targets has shown a low stability of these triplexes, especially for those formed by (G,T)-oligonucleotides [22, 25]. This situation changes dramatically when the (G,A)- and (G,T)-triplex forming sequences are connected to the appropriate oligopurine Watson-Crick sequences to form hairpins or cyclic oligonucleotides designed to bind single-stranded polypyrimidide targets. In this situation, the differences observed with (G,T)- antiparallel triplexes disappear and (G,A)- and (G,T)-antiparallel triplexes have equally high stability. Although this behaviour has been described previously [10, 11, 16, 28], very little biological data has been generated using this potentially powerful strategy.

Most of the prior work using cyclic oligonucleotides for triplex formation has been performed with C-/T-rich oligonucleotides [8, 9]. These oligonucleotides target the polypurine sequence by forming parallel triplexes that are stable at acidic pH. We chose to target the

complementary polypyrimidine sequence as a result of recent developments using 8-aminopurines. Recently, we have shown that substitution of guanine with 8-aminoguanine results in strong stabilization of antiparallel triplexes [16]. We believe that the introduction of 8-aminoguanine in cyclic oligonucleotides will be of interest in order to further increase the binding affinities. Nevertheless, even with the use of natural nucleosides we demonstrate that by using cyclic and hairpin oligonucleotides it is possible to achieve much stronger binding than with regular duplex recognition at neutral pH.

This study was supported by the Dirección General de Investigación Científica (BQU2003-00397 and BFU2004-02048/BMC), the Generalitat de Catalunya (2001-SGR-0049) and Fundació La Caixa (BM04-52-0). We thank Drs Jordi Robles, Anna Grandas, Enrique Pedroso and Vicent Marchán for their help in the preparation of the oligonucleotides and the use of the Meltwin program. We thank *Waters* for their support in the use of XTerra® HPLC columns.

Experimental Part

General. Phosphoramidites and ancillary reagents used during oligonucleotide synthesis were from *Applied Biosystems* (USA), *Transgenomic* (Scotland), *Link Technologies* (Scotland) and *Glen Research* (USA). The rest of the chemicals were purchased from *Aldrich, Sigma* or *Fluka*. Long chain amino-controlled pore glass (LCAA-CPG) was purchased from CPG (USA). Solvents were from *S.D.S*. (France). NAP-10 columns (Sephadex G-25) were purchased from *Amersham*. Solid support for the preparation of 3'-phosphorylated precursors was synthesized as described elsewhere [17].

Instrumentation. Oligonucleotide sequences were synthesized on a *Applied Biosystems* DNA synthesizer model 392. UV-Visible spectra were recorded on a *Shimadzu* UV-2101PC and CD spectra on a *Jasco* J810.

Oligonucleotide Synthesis. Oligonucleotides were prepared using standard (benzoyl- or isobutyryl-protected) 3'-[(2'-cyanoethyl)phosphoramidites] and the phosphoramidite of (4,4'-dimethoxytrityloxyethyl) hydroxyethyl sulfone [17]. Supports were obtained from commercial sources or prepared as described elsewhere [17].

After the assembly of the sequences in batches of 1 μmol or 200 nmols, the resulting supports were treated with 1ml of concentrated ammonia (overnight at 55ºC). Oligonucleotide supports carrying a phosphate group at the 3'- end were treated overnight with 1ml of 1:1 mixture of 40% methylamine and 32% NH_3 in *aqueous* solutions.

The products arising from ammonia treatment were dissolved in water and purified by HPLC using a PRP-1 10 μm column (305 x 7mm, *Hamilton*, USA) at a flow rate of 3 ml/min. A 20min linear gradient from 15 to 50% acetonitrile over 100mM aqueous triethylammonium acetate was used for oligonucleotides carrying the $(MeO)_2$-Tr group. After removal of the $(MeO)_2$-Tr group with 80% acetic acid (30min) the resulting oligonucleotides were purified on the same column using a 20min linear gradient from 5 to 25% acetonitrile over 100 mM aqueous triethylammonium acetate.

5'-Phosphorylated and cyclic oligonucleotides were purified by HPLC using an XTerra® MS C18 2.5 μm (*Waters,* USA) column: flow rate 1 ml/min; column temperature, 60 ºC. A 20 min gradient from 5 to 15% acetonitrile over 100 mM aqueous triethylammonium acetate was used. Yields after purification: **1-4** (1 μmols), 20-40 OD units. MS (MALDI-TOF) of oligonucleotide **5**, 9412.7 (M) expected for $C_{300}H_{374}N_{111}O_{186}P_{29}$ 9410.2; oligonucleotide **6**: 9459.6 (M) expected for $C_{300}H_{369}N_{126}O_{176}P_{29}$ 9455.3; oligonucleotide **1**, 9492.8 (M) expected for $C_{300}H_{375}N_{111}O_{189}P_{30}$ 9490.2; oligonucleotide **2**, 9537.8 (M) expected for $C_{300}H_{370}N_{126}O_{179}P_{30}$ 9535.3.

Cyclization of oligonucleotides.

Carbodiimide activation. Phosphorylated linear precursors **1-4** (4 OD units) and template **14** (1.3 OD units) were dissolved on 0.14 ml of the following buffer : 50 mM morpholinoethansulfonic acid (MES) pH 6.0, 20 mM $MgCl_2$. The solution was heated at 80ºC followed by slow cooling at room temperature. Solid water-soluble carbodiimide (EDC) was added to obtain a 0.25 M EDC solution and the resulting mixture was kept at 4ºC for 16-20 hours. The resulting solution was dialyzed against water and then concentrated and purified by HPLC using an XTerra® column (see conditions above, *Figure 2*). Yield: **7**, 0.3-0.6 OD units; **8**, 2-3 OD units. MS (MALDI-TOF) of sequence **8**: 9525.6 (M) expected for $C_{300}H_{368}N_{126}O_{178}P_{30}$ 9517.3.

BrCN activation. Phosphorylated linear precursors **1-4** (4 O.D. units) and template **14** (1.3 OD units) were dissolved in0.5 ml of the following buffer: 200 mM imidazol-HCl pH 7.0, 100 mM $NiCl_2$. BrCN (0.062 ml of a 5M solution in acetonitrile) was added to obtain a 125 mM BrCN solution and the resulting mixture was kept 4 ºC for 16-20 hours. The solution was then centrifuged and the supernatant dialyzed against water. Finally, the supernatant was concentrated and analyzed by gel electrophoresis indicating that contain only the 11bases template **14**, so it was discarded. The pellet was treated with 0.25 ml of 0.1 M EDTA and 0.25 ml of water. The resulting solution was dialyzed against water and then concentrated and purified by PAGE yielding 0.5 O.D. units for **7** and 0.6 O.D. units for **8**.

*Melting experiments***.** Melting experiments were performed by mixing equimolar amounts of the appropriate oligonucleotides dissolved in a soln. containing 50 mM $MgCl_2$, 10 mM sodium cacodylate (pH 7.2), and 0.1 mM EDTA. Oligonucleotides were annealed by slow cooling from 90 ºC to room temperature. UV Absorption spectra and melting curves (absorbance vs temperature) were recorded in 1-cm path-length cells using a *Shimadzu* UV2101PC UV/VIS spectrophotometer

(Japan) with a temperature controller using a programmed temperature increase of 0.5˚/min. Melting curves were obtained by monitoring the absorbance at 260 nm of triplex concentrations of approx. 2-4 μM. All of the absorbance *vs*. temperature plots showed sigmoidal curves, indicating cooperative transition, and the data were fitted to a two-state model using MeltWin 3.5 software [29] in order to determine Tm and ΔG values. Thermodynamic data were calculated as mean values of three independent melting experiments. Results: see *Table 2* and *3*.

CD melting experiments

The same solutions used for UV experiments were used for CD spectroscopy. All CD measurements were performed on a *Jasco* Spectropolarimeter (model J810) equipped with a thermostat-controlled cell holder with a cell path length of 1 cm. Melting experiments were determined using steps of 5 ^{o}C followed by 5 min equilibration time, and a temperature ramp of 1 ^{o}C per minute.

Data treatment

The complete CD spectra recorded during melting experiments were analyzed by means of the multivariate curve resolution (MCR) method [22, 26]. This method, which is based on factor analysis, has been widely applied to the analysis of spectroscopic data recorded from conformational studies of nucleic acids and proteins [27], and only a brief description is given here. The reader is referred to references [22, 26, 27] for more information about the procedure and its applications. The goal of this method is the recovery of information about the number of species, and their concentration and spectral profiles. This is performed using the experimental spectra without the postulation of a physico-chemical model. For this purpose, the complete experimental CD spectra recorded during a melting experiment are collected in a table or matrix **D**. The dimensions of **D** were *Nr* rows x *Nm* columns, where *Nr* are the spectra recorded at successive

temperature values and *Nm* the number of wavelengths measured in each spectrum. The matrix **D** is analyzed according to the MCR procedure to obtain information about the thermodynamic behavior of the system. For melting experiments, the information consisted of the number of conformations, their concentration profiles (and the corresponding Tm values), and the pure spectrum for each one of them. Mathematically, the experimental data model can be written as:

$$\mathbf{D} = \mathbf{C}\,\mathbf{S}^{\mathbf{T}} + \mathbf{E} \qquad \text{(equation 1)}$$

where **C** is the data matrix containing the concentration profiles, $\mathbf{S}^{\mathbf{T}}$ is the pure spectrum and **E** is the residual noise not explained by the species or conformations in **C** and $\mathbf{S}^{\mathbf{T}}$.

All MCR-ALS calculations were performed using in-house MATLAB® (version 6; The Mathworks Inc, Natick, MA) routines.

REFERENCES

[1] N.T. Thuong, C. Hélène *Angew. Chem. Int. Ed. Engl.*, **1993**, *32*, 666-690.

[2] P.P. Chan, P.M. Glazer *J. Mol. Med.*, **1997**, *75*, 267-282.

[3] V.N. Soyter, V.N. Potoman, *Triple-helical Nucleic Acids.* Springer-Verlag, New York, N.Y. **1996**.

[4] C. Giovannangeli, T. Montenay-Garestier, M. Rouge, M. Chassignol, N.T. Thuong, C. Hélène, *J. Am. Chem. Soc.,* **1991**, *113*, 7775-7776.

[5] G. Prakash, E.T. Kool, *J. Chem. Soc. Chem. Commun.*, **1991**, *646*, 1161-1162.

[6] P.E. Nielsen, M. Egholm, R. Berg, O. Buchardt, *Science* **1991**, *254*, 1497-1500.

[7] H. Kuhn, V.V. Demidov, P.E. Nielsen, M.D. Frank-Kamenetskii, *J. Mol. Biol.,* **1999**, *286*, 1337-1345.

[8] E.T. Kool, *Chem Rev.*, **1997**, *97*, 1473-1478

[9] E. T. Kool, *Annu. Rev. Biophys. Biomol. Struct.,* **1996**, *25*, 1-28.

[10] S. Wang, E.T. Kool, *J. Am. Chem. Soc.,* **1994**, *116*, 8857-8858.

[11] T. Vo, S. Wang, E.T. Kool, *Nucleic Acids Res.,* **1995**, *23*, 2937-2944.

[12] A. Miksimenko, E.V. Volkov, J.R. Bertrand, H. Porumb, C. Malvy, Z.A. Shabarova, M. B. Gottlikh, *Eur. J. Biochem.,* **2000**, *267*, 3592-3603.

[13] L.E. Xodo, G. Manzini, F. Quadrifolio, G.A. van der Marel, J.H. van Boom, *Nucleic Acids Res.,* **1991**, *19*, 5625-5631.

[14] G. Manzini, L.E. Xodo, D. Gasparotto, *J. Mol. Biol.,* **1990**, *213*, 833-843.

[15] A. Aviñó, M. Frieden, J.C. Morales, B. G. de la Torre, R. Güimil-García, F. Azorín, J.L. Gelpí, M. Orozco, C. González, R. Eritja. *Nucleic Acids Res.,* **2002**, *30*, 2609-2619.

[16] A. Aviñó, E. Cubero, C. González, R. Eritja, M. Orozco, *J. Am. Chem. Soc.,* **2003**, *125*, 16127-16138.

[17] T. Horn, M.S. Urdea, *Tetrahedron Lett.* **1986**, *27*, 4705-4708.

[18] A. MacMillan, G.L. Verdine, *Tetrahedron* **1991**, *47*, 2603-2616.

[19] M.P. Reddy, F. Farooqui, N.B. Hanna, *Tetrahedron Lett.,* **1996**, *37*, 8691-8694.

[20] N.G. Dolinnaya, M. Blumenfeld, I.N. Merenkova, T. S. Oretskaya, N.F. Krynetskaya, M.G. Ivanovskaya, M. Vasseur, Z.A. Shabarova, *Nucleic Acids Res.,* **1993**, *21*, 5403-5407.

[21] D. Murphy, R. Eritja, G. Redmond, *Nucleic Acids Res.,* **2004**, *32*, e65.

[22] J. Jaumot, A. Aviñó, R. Eritja, R. Tauler, R. Gargallo, *J. Biomol. Str. Dyn.,* **2003**, *21*, 267-278.

[23] J.L. Mergny, L. Lacroix, *Oligonucleotides*, **2003**, *13*, 515-537.

[24] V. Dapic, V. Abdomerovic, R. Marrington, J. Peberdy, A. Rodger, J.O. Trent, P. J. Bates, *Nucleic Acids Res*., **2003**, *31*, 2097-2107.

[25] Y. He, P.V. Scaria, R.H. Shafer, *Biopolymers*, **1997**, *41*, 431-441.

[26] MCR routines for Matlab® and tutorials are freely available at the web site: www.ub.es/gesq/mcr/mcr.htm

[27] J. Jaumot, M. Vives, R. Gargallo, *Anal. Biochem.* **2004**, *327*, 1-13.

[28] M. Mills, P.B. Arimodo, L. Lacroix, T. Garestier, C. Hélène, H. Klump, J.L. Mergny, *J. Mol. Biol*.. **1999**, *291*, 1035-1054.

[29] J.A. McDowell, D.H. Turner, *Biochemistry*, **1996**, *35*, 14077-14089.

Table 1: *Oligonucleotides Prepared in this Study*

Number	Sequence
1	5'-phosphate-AGGAGA-T_4-TGTGGTGGTTG-T_4-GAAGG-3'
2	5'-phosphate-AGGAGA-T_4-AGAGGAGGAAG-T_4-GAAGG-3'
3	5'-AGGAGA-T_4-TGTGGTGGTTG-T_4-GAAGG-phosphate-3'
4	5'-AGGAGA-T_4-AGAGGAGGAAG-T_4-GAAGG-phosphate-3'
5	5'-AGGAGA-T_4-TGTGGTGGTTG-T_4-GAAGG-3'
6	5'-AGGAGA-T_4-AGAGGAGGAAG-T_4-GAAGG-3'
7	*Cyclo*-(5'-AGGAGA-T_4-TGTGGTGGTTG-T_4-GAAGG-3')
8	*Cyclo*-(5'-AGGAGA-T_4-AGAGGAGGAAG-T_4-GAAGG-3')
9	5'-GAAGGAGGAGA-T_4-TGTGGTGGTTG-3'
10	5'-GAAGGAGGAGA-T_4-AGAGGAGGAAG-3'
11	5'-GAAGGAGGAGA-T_4-GTGTGGTTTGT-3'
12	5'-GAAGGAGGAGA-T_4-GAGAGGAAAGA-3'
13	5'-GAAGGAGGAGA-3'
14	5'-TCTCCTCCTTC-3'

Table 2: *Melting Temperatures (T_m, ºC) and Free Energies (ΔG_{37}, Kcal/mol) for Complexes Formed by Oligonucleotides Carrying (G,A)-Hoogsteen Strand* (**2, 4, 6, 8, 10**) *and Control Oligonucleotides* (**12, 13**) *with the Pyrimidine Target Sequence* **14**.

Ligand	Complex	T_m [ºC], UV[a,b])	ΔG_{37}, UV[a,b])	T_m [ºC], CD[a,b])
8	TCTCCTCCTTC AGAGGAGGAAG AGAGGAGGAAG	59.0	-19.1	51.5
6	TCTCCTCCTTC AGAGGA GGAAG AGAGGAGGAAG	57.3	-17.5	52
4	TCTCCTCCTTC AGAGGA pGGAAG AGAGGAGGAAG	58.1	-17.5	n.d.
2	TCTCCTCCTTC AGAGGAp GGAAG AGAGGAGGAAG	55.6	-15.2	n.d.
10	TCTCCTCCTTC AGAGGAGGAAG AGAGGAGGAAG	60.9	-15.5	n.d.
12	TCTCCTCCTTC AGAGGAGGAAG GAGAGGAAAGA	49.4	-10.8	n.d.
13	TCTCCTCCTTC AGAGGAGGAAG	48.5	-11.2	n.d.

[a]) 0.050M $MgCl_2$, 0.01M sodium cacodylate pH 7.2, 0.1mM EDTA. [b]) Uncertainties in Tm values and in free energies are estimated at 1 ºC, and 15%. n.d.: not determined.

Table 3: *Melting Temperatures and Free Energies of Complexes Formed by Oligonucleotides Carrying (G,T)-Hoogsteen Strand* (**3, 5, 7, 9**) *and Control Oligonucleotide* **11** *with the Pyrimidine Target Sequence* **14**.

Ligand	Complex	T_m [ºC], UV[a,b])	$\Delta G_{37°}$, UV [a,b])
7	TCTCCTCCTTC AGAGGAGGAAG TGTGGTGGTTG	56.5	n.a.
5	TCTCCTCCTTC AGAGGA GGAAG TGTGGTGGTTG	55.9	-17.6
3	TCTCCTCCTTC AGAGGA pGGAAG TGTGGTGGTTG	54.9	-15.7
1	TCTCCTCCTTC AGAGGAp GGAAG TGTGGTGGTTG	51.6	-14.7
9	TCTCCTCCTTC AGAGGAGGAAG TGTGGTGGTTG	58.5	-15.4
11	TCTCCTCCTTC AGAGGAGGAAG GTGTGGTTTGT	49.5	-11.2

[a]) 50mM $MgCl_2$, 10 mM sodium cacodylate pH 7.2, 0.1mM EDTA. [b]) Uncertainties in Tm values and in free energies are estimated at 1 ºC, and 15 %. n.a.: not possible to analyze.

LEGENDS

Scheme 1. *Strategies for binding nucleic acids by triplex formation*. (left) Strategy for targeting duplexes using triplex-forming oligonucleotides (TFO). (center and right) Targeting single-stranded polypyrimidine nucleic acid sequences by triplex formation using hairpins (centre) or cyclic oligonucleotides (right) made by linking the polypurine strand with the triplex forming strand (TFO). A similar approach has been used for targeting the polypurine sequence (see ref. [8,9]).

Scheme 2. *Triplexes analyzed in this study made of the pyrimidine target sequence with cyclic oligonucleotides formed by linking the Watson-Crick purine strand and the (G,A)- or (G,T)-antiparallel strand.* The phosphate bond that was selected to disconnect the cyclic oligonucleotide occurs between the G and the A shown in bold. Sequences of the linear precursors are shown in *Table 1*.

Figure 1: *HPLC Analysis of 5'-phosphorylated oligonucleotide **2** using an XTerra® column*. The figure shows the HPLC profile of the crude product obtained after ammonia treatment. Fractions I and II contained the desired phosphorylated oligonucleotide and the unphosphorylated oligonucleotide respectively.

Figure 2: *HPLC profile of the product obtained in template-assisted cyclization of **2**, analyzed using an XTerra® column*. (a) cyclization of sequence **1** and (b) cyclization of sequence **2**. Fractions I and II contained the starting phosphorylated oligonucleotide (**1** or **2**) and the desired cyclic oligonucleotide (**7** or **8**), respectively. The peak eluting close to 10 min correspond to template sequence **14**.

Figure 3. CD-spectra of cyclic oligonucleotide **8** with and without target sequence **14** (0.050M $MgCl_2$, 0.01M sodium cacodylate pH 7.2, 25 ºC, 3 μM triplex concentration).

Figure 4. Thermal denaturation of triplex formed by cyclic oligonucleotide **8** with target sequence **14** followed by CD-spectroscopy. (0.050M $MgCl_2$, 0.01M sodium cacodylate pH 7.2, 0.1mM EDTA, 3 μM triplex concentration). A) Experimental spectra recorded from 20 to 80 ^{o}C, at 5 ^{o}C intervals (matrix **D**). B) MCR-resolved concentration profiles according to Equation 1 (matrix **C**). C) MCR-resolved pure spectra (matrix $\mathbf{S^T}$). (a) triplex, (b) unfolded species.

Scheme 1

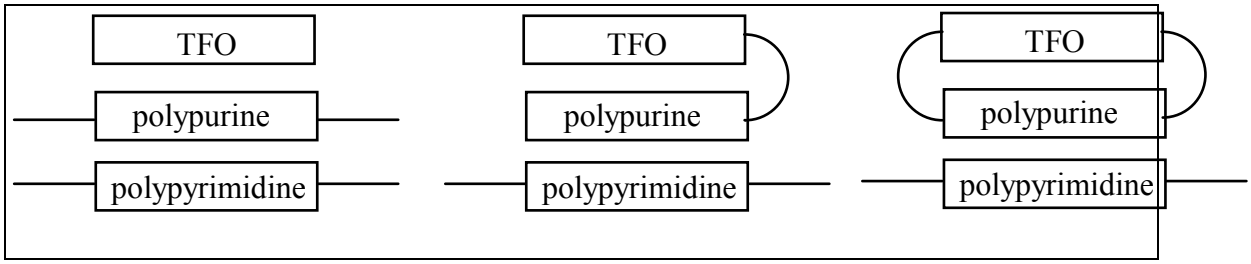

Scheme 2

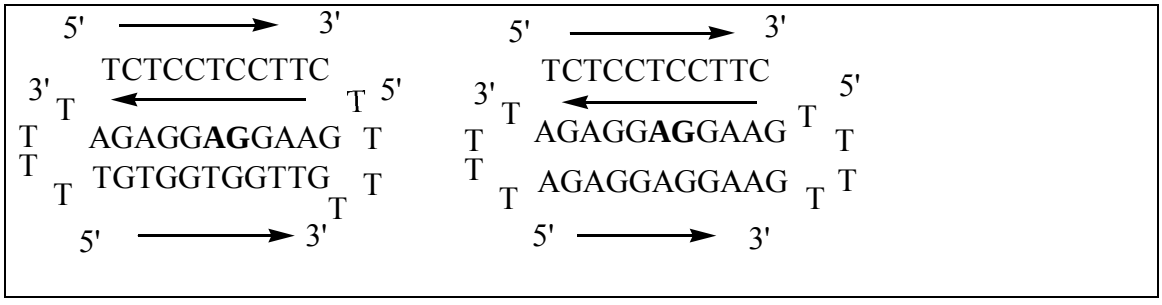

Figure 1

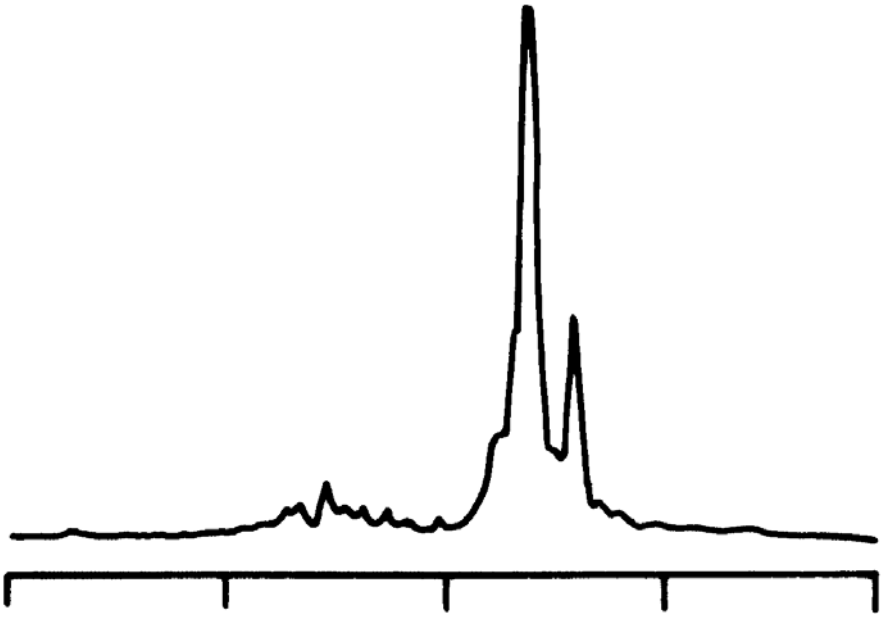

Figure 2

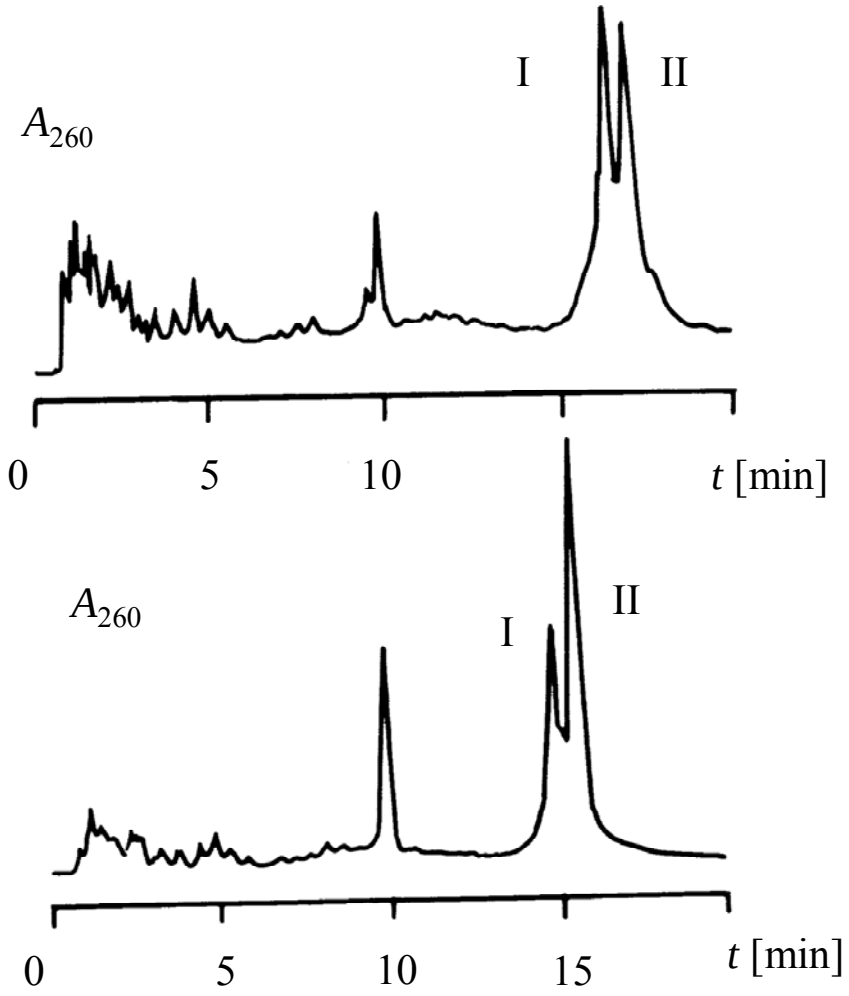

Figure 3

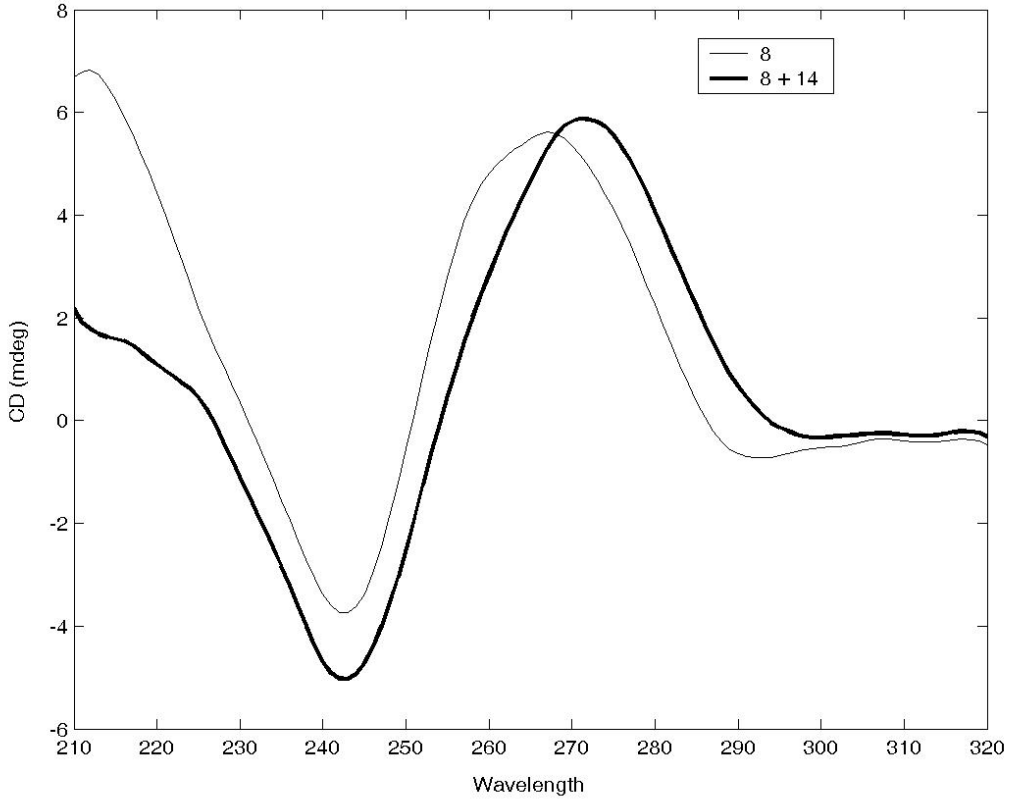
8
8 + 14
CD (mdeg)
Wavelength
8
6
4
2
0
-2
-4
-6
210
220
230
240
250
260
270
280
290
300
310
320

Figure 4

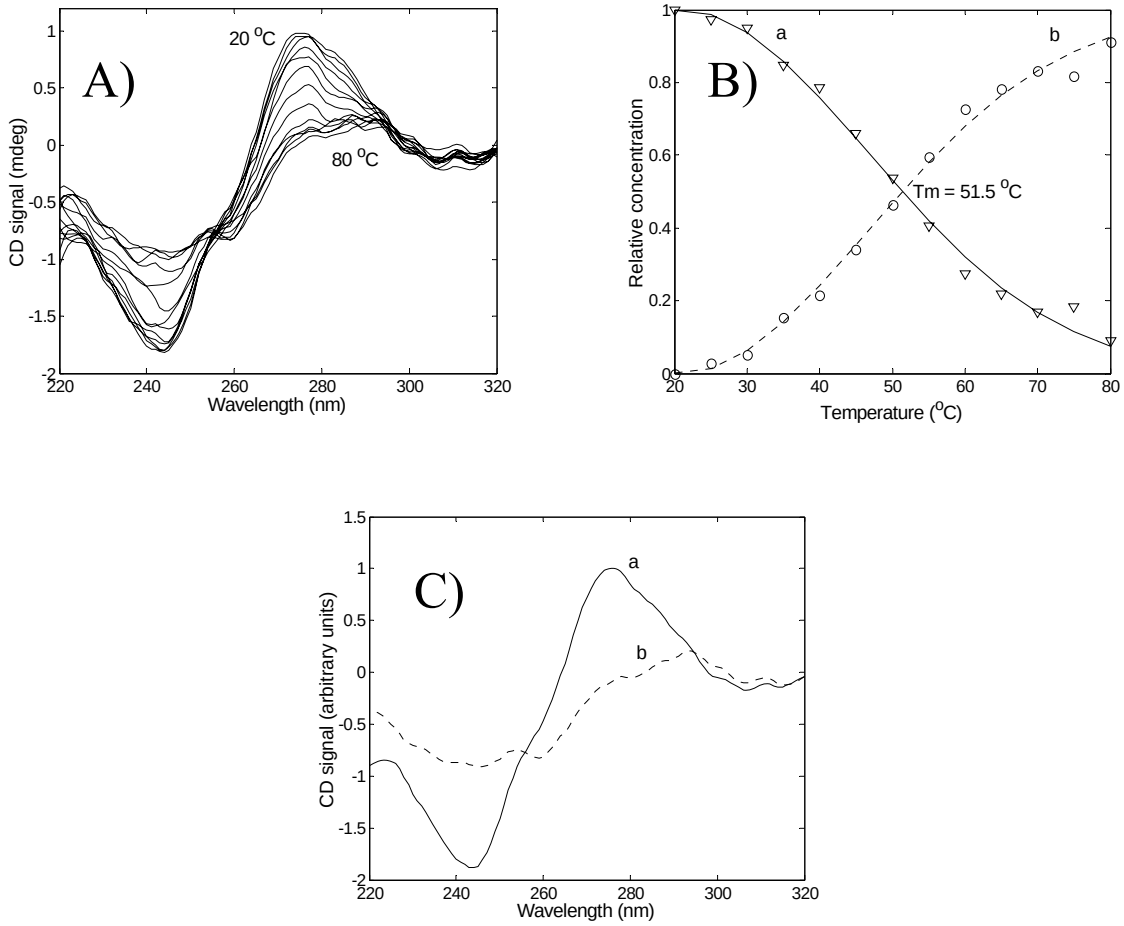
A)
20 °C
80 °C
CD signal (mdeg)
Wavelength (nm)
B)
a
b
Tm = 51.5 °C
Relative concentration
Temperature (°C)
C)
a
b
CD signal (arbitrary units)
Wavelength (nm)